

## Dipole matrix elements and the nature of charge oscillation under coherent interband excitation in quantum wells

R. A. Coles, R. A. Abram, and S. Brand

*Department of Physics, University of Durham, Durham DH1 3LE, United Kingdom*

M. G. Burt

*BT Laboratories, Martlesham Heath, Ipswich, Suffolk IP5 3RE, United Kingdom*

(Received 2 October 1998)

An empirical pseudopotential method is used to model two type-I quantum-well systems, allowing the investigation of interband dipole-matrix elements and charge oscillation under coherent optical excitation. Each relevant (microscopically varying) wave function is expressed as an exact envelope-function expansion to which various approximations are made, in analogy with envelope-function methods such as the  $\mathbf{k}\cdot\mathbf{p}$  model. The approximation to the quantum-well energy eigenfunctions of a single envelope function multiplying a band-edge zone-center state, the “atomic picture,” is shown to underestimate by orders of magnitude the interband dipole-matrix element. Including terms due to the second band edge, which play only a minor role in the exact envelope-function expansion, provides a good approximation to the true dipole-matrix element, which is significantly greater than the atomic picture predicts. In addition, the effect on the interband charge oscillation of omitting the second band-edge terms is shown to be a reduction of the oscillation from the width of the well to the atomic scale. These results confirm that the earlier results of Burt hold for realistic three-dimensional systems. [S0163-1829(99)03343-3]

The rate of an optically induced electron transition between a pair of quantum-well states can be expressed in terms of the matrix element between the states of either the dipole moment or the momentum. Consideration of the former has the attraction that the factors that determine the value of the matrix element are apparently easier to appreciate in physical terms. Since, at least for wide wells, a quantum-well bound state in band  $j$  can apparently be reasonably approximated by the product of a slowly varying envelope function and the periodic part of the  $j$ th band-edge Bloch function, we expect a large intraband dipole-matrix element between the ground and first excited state, by analogy with  $s$  to  $p$  atomic transitions, since the envelope functions of the ground and first excited states in a quantum well have  $s$ - and  $p$ -like symmetry, with respect to the center of the well. The same approximation suggests a small interband matrix element between valence- and conduction-band ground states due to the similar nature of the envelope functions for the two states, the main differences being between the Bloch periodic parts which are characteristic of the atomic scale. However, Burt<sup>1-3</sup> has shown this “atomic picture” to be incorrect for quantum wells and illustrated the point with examples based on simple models of quantum-well structures.

The purpose of this paper is to test Burt’s conclusions for real quantum-well systems, to which end a model employing a local empirical pseudopotential method<sup>4,5</sup> (EPM) is used. This allows the generation of a full-zone band structure, with spin-orbit coupling effects included. To determine the bound states for a quantum well, the band structure for a complex wave vector<sup>6,7</sup> is first calculated for each material, using an 89 plane-wave basis to ensure satisfactory convergence of energies and wave functions.

A technique has been developed (to be submitted for pub-

lication) for the extraction of envelope functions, as defined by Burt,<sup>8</sup> from the EPM wave function. These envelope functions are by definition continuous *and* smooth at all positions, including across the interfaces between barrier and well materials. The valence- and conduction-band bound states, with wave functions  $\psi^{(v)}$  and  $\psi^{(c)}$ , respectively, can be expressed as envelope-function expansions using bulk zone-center states  $u_n(\mathbf{r})$  as the basis, i.e.,

$$\psi^{(j)}(\mathbf{r}) = \sum_n F_n^{(j)}(\mathbf{r})u_n(\mathbf{r}), \quad (1)$$

where  $n$  is the band index,  $F_n$  are the envelope functions, and  $j$  labels the bound state, indicating in which band (conduction or valence) the bound state exists. The wave function and zone-center states are both spinors, while the envelope functions are scalars (the dependence on the spatial coordinate  $\mathbf{r}$  will not be made explicit in the subsequent discussion unless its omission might lead to confusion). Equation (1) is valid in both barrier and well layers for a given choice of  $u_n$  fixed throughout the structure, which can be chosen to be barrier or well bulk zone center states, as normally used in  $\mathbf{k}\cdot\mathbf{p}$  calculations, or some other appropriate complete set.

However, the envelope functions depend on the particular choice made, the well material zone-center states being used in the present work. It is important to note that the expansion given in Eq. (1) is exact and fully reproduces the (pseudo) wave function (though of course the numerical calculations are necessarily approximate).

Two quantum-well systems are modeled, with the well growth direction being  $z$  and the in-plane wave vector  $\mathbf{k}_{\parallel}$  set to zero. The two systems are the widely studied

TABLE I. Details of the two quantum-well systems considered (modeled at room temperature).  $\Delta E_v$  and  $\Delta E_c$  are the valence- and conduction-band offsets (Refs. 9,14,15), respectively.

Barrier	InP	CdTe
Well	$\text{In}_{0.53}\text{Ga}_{0.47}\text{As}$	InSb
$\Delta E_v$ (eV)	0.380	0.870
$\Delta E_c$ (eV)	0.222	0.390
Well $E_g$ (eV)	0.753	0.180
Well width ( $\text{\AA}$ )	80.696	153.9

InP/ $\text{In}_{0.53}\text{Ga}_{0.47}\text{As}$  system, where the ternary alloy is lattice matched to bulk InP with  $a = 5.8688 \text{ \AA}$ ,<sup>9</sup> and the less well-known CdTe/InSb system, which is treated here as lattice matched with the CdTe lattice constant of  $a = 6.480 \text{ \AA}$ ,<sup>5</sup> although in fact InSb is very slightly mismatched with  $a = 6.478 \text{ \AA}$ .<sup>5</sup> A virtual crystal model is used to represent the alloy. The important parameters for both systems are summarized in Table I. The InSb and  $\text{In}_{0.53}\text{Ga}_{0.47}\text{As}$  wells are 55 and 95 atomic layers wide, respectively, where an atomic layer is a single plane of atoms with a quarter of the width of the lattice constant.

The typical nature of the envelope functions is illustrated in Fig. 1, which shows plots of the significant contributions for one of the spin degenerate pairs of conduction-band ground states of the InP/ $\text{In}_{0.53}\text{Ga}_{0.47}\text{As}$  system. Due to the inclusion of spin, there are two zone-center states for each of the conduction, heavy-hole (hh), light-hole (lh), and spin split-off (sso) bands, but for clarity the envelope functions corresponding to just one of these are plotted and their phases have been adjusted so that they are real. They take the same form as seen in the results of a typical eight band  $\mathbf{k} \cdot \mathbf{p}$  method.<sup>10–12</sup> Since the  $u_n$  are normalized to the unit cell, it is apparent from the relative values of the envelope functions that the expansion for  $\psi^{(c)}$  is dominated by the term associated with the zone-center state for the first conduction band, i.e., in general the dominant term is that due to the zone-center state for the band which forms the quantum well in which the state is confined. For example, the contribution from the conduction-band term to the total charge density of the conduction-band ground state of the InP/ $\text{In}_{0.53}\text{Ga}_{0.47}\text{As}$  system is 97%. This is the justification for the single-band-edge (SBE) approximation, which takes the energy eigenfunctions to be of the form

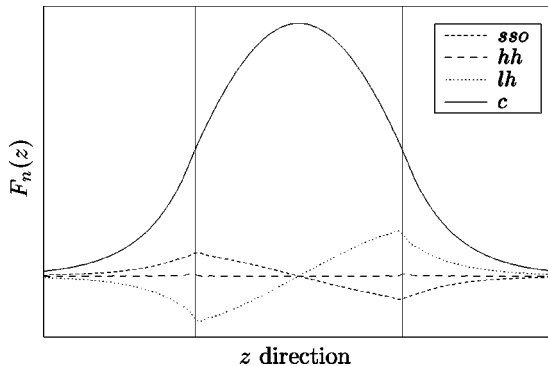


FIG. 1. The  $z$  dependence of the significant  $F_n$  for an electron ground state at  $\mathbf{k}_{\parallel} = (0,0)$ . The locations of the well walls are indicated by vertical lines.

TABLE II. Magnitude of selected dipole-matrix elements, in  $e\text{\AA}$ , using the three expressions for the wave functions discussed in the text. The states are characterized according to the band with the dominant contribution to the envelope-function expansion, while the subscripts indicate ground or first excited state (1 or 2, respectively).

System	Method	$c_1\text{-hh}_1$	$c_1\text{-lh}_1$	$c_1\text{-}c_2$
InP/ $\text{In}_{0.53}\text{Ga}_{0.47}\text{As}$	SBE	$4 \times 10^{-9}$	$1 \times 10^{-8}$	15.431
	DBE	$2 \times 10^{-5}$	4.807	15.751
	exact	$5 \times 10^{-4}$	4.819	15.793
CdTe/InSb	SBE	$1 \times 10^{-7}$	$1 \times 10^{-6}$	22.692
	DBE	0.003	13.586	24.266
	exact	0.002	13.643	24.362

$$\psi^{(j)} \approx F_j^{(j)} u_j, \quad (2)$$

where  $j = v$  or  $c$ , which has been widely used to predict the electronic and optical properties of quantum wells (see, for example, Ref. 13).

The dipole-matrix element (in units of the electronic charge) between states  $\psi^{(i)}$  and  $\psi^{(j)}$  along the well growth direction  $z$  is given by

$$z_{ij} = \langle \psi^{(i)} | z | \psi^{(j)} \rangle. \quad (3)$$

The dipole-matrix elements between selected states predicted by this approximation are listed in Table II.

The valence–conduction-band entries in the SBE approximation represent the ‘‘atomic dipole approximation,’’<sup>2,3</sup> where interband transitions between states with the same envelope-function symmetry but different zone-center states have a very small dipole-matrix element. On the other hand, the intraband dipole-matrix element between states dominated by the same zone-center terms but whose envelopes are of opposite parity can have dipole moments much larger than the atomic scale. Indeed, the intraband dipole moment for the CdTe/InSb system is approximately  $24e \text{ \AA}$ , which corresponds to a displacement of the electronic charge of about 16% of the well width, which is a factor of roughly four greater than the lattice parameter ( $6.48 \text{ \AA}$ ), or 8.5 times the bond length.

We now examine the dipole-matrix elements as predicted by a double-band-edge (DBE) approximation, given by

$$\psi^{(j)} \approx F_v^{(j)} u_v + F_c^{(j)} u_c, \quad (4)$$

where the subscript  $v$  implicitly includes a sum over hh, lh, and sso bands. Inclusion of the sso band, which is not strictly at the band edge, is not essential to the present discussion but improves the accuracy of the approximation due to its coupling with the conduction band. The predicted dipole matrix elements are shown in Table II, as are those using the full complex band-structure EPM wave function, or equivalently, the complete expansion in Eq. (1). While the intraband dipole-matrix elements differ only slightly between the two

approximations and the exact calculation as might be expected, for the interband cases there are major differences between the single- and double-band-edge approximations, the latter being in good agreement with the exact result. For the electron to light-hole case, the inclusion of the second band-edge terms has increased the matrix element by at least 6 orders of magnitude. For the CdTe/InSb system, the interband matrix element is actually about  $13.6e \text{ \AA}$ , corresponding to 9% of the well width, which is clearly at odds with the atomic approximation. It is also important to point out that the failure of the SBE approximation for the interband dipole-matrix elements does not imply that the same problem occurs for the interband momentum matrix elements, which are actually predicted rather well in that approximation.

Obviously, the single-band-edge approximation has omitted detail vital to the correct evaluation of the interband dipole-matrix elements. This turns out to be the contribution of the ‘cross’ terms,<sup>3</sup>

$$\langle F_v^{(c)} u_v | z | F_v^{(v)} u_v \rangle + \langle F_c^{(c)} u_c | z | F_c^{(v)} u_c \rangle, \quad (5)$$

which dominate the interband matrix element, even though they derive from terms which play only a minor role in the envelope-function representation of the wave function. The terms in Eq. (5) have similar features to those with intraband matrix elements in the single-band-edge approximation, i.e., a common zone-center state and envelopes of differing parity. Thus, large dipole-matrix elements are obtained.

Related to the dipole-matrix element between bound states is the charge oscillation induced by coherent optical excitation of an electron between the two states, due to illumination by a laser, for example. Under such conditions, we expect to see charge oscillation on the scale of the matrix element. Hence, for interband excitation, the single-band-edge approximation predicts atomic scale charge oscillation.

We consider at time  $t_0$  the electron to be in a superposition with an equal amplitude of valence- and conduction-band bound states, i.e.,

$$\Psi(\mathbf{r}, t_0) = \frac{1}{\sqrt{2}} [\Psi^{(v)}(\mathbf{r}, t_0) + \Psi^{(c)}(\mathbf{r}, t_0)], \quad (6)$$

where  $\Psi^{(j)}(\mathbf{r}, t) = \psi^{(j)}(\mathbf{r}) e^{-i\omega_j t}$  is the (normalized) solution to the time-dependent Schrödinger equation for bound state  $j$ . Therefore, at a later time  $t$ , the charge density  $|\Psi(\mathbf{r}, t)|^2$  will have a time-dependent component  $\tau(\mathbf{r}, t)$  given by

$$\tau(\mathbf{r}, t) = \frac{1}{2} \{ (\psi^{(v)})^* \psi^{(c)} e^{-i\omega_c t} + \text{c.c.} \}, \quad (7)$$

where  $\omega_{cv} = \omega_c - \omega_v = (E_c - E_v)/\hbar$  gives the angular frequency of oscillation. Figure 2 shows plots of  $\tau$  for light-hole to conduction-band ground states in the InP/In<sub>0.53</sub>Ga<sub>0.47</sub>As system, as calculated using the two approximations and the exact model using the complex wave-vector band-structure method. After half a period of oscillation,  $\tau$  has the same form as in Fig. 2 but is reflected about the center of the

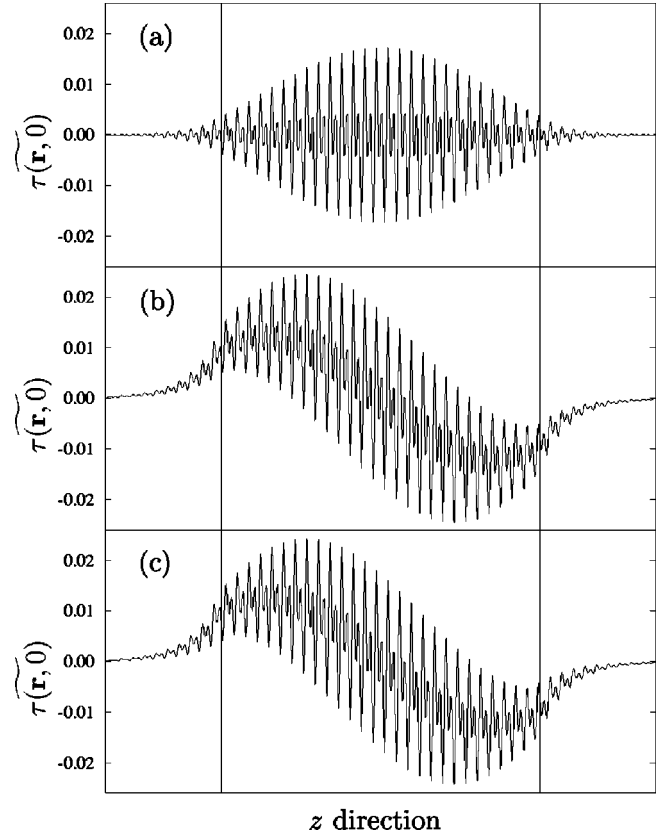


FIG. 2. In-plane averaged value of the time-dependent component,  $\tau(\mathbf{r}, 0)$ , of the oscillatory charge density between light-hole and conduction-band ground states in the InP/In<sub>0.53</sub>Ga<sub>0.47</sub>As system at time  $t=0$ . (a) Single-band-edge approximation, (b) double-band-edge approximation, (c) exact complex band-structure calculation.

quantum well. Thus, the double-band-edge approximation and the exact calculation of  $\tau$ , Figs. 2(b) and 2(c), will lead to the charge density being modulated over the width of the well. However, the single-band-edge approximation only modulates the charge density on the scale of the crystal unit cell and predicts a form for  $\tau$  that has a symmetric envelope about the center of the well.

Thus it is apparent that, as is the case when predicting interband dipole-matrix elements, the inclusion of the subdominant terms in the envelope-function expansion of the wave function is crucial in establishing interband charge oscillation on the scale of the well. In the single-band-edge (dominant band) approximation,  $\tau(\mathbf{r}, 0)$  reduces to  $(F_v^{(v)})^* F_c^{(c)} u_v^* u_c$ , plus its complex conjugate. The envelope functions have the same parity, so that their product has even parity, with respect to the center of the well. Thus,  $\tau$  can only produce charge oscillations on the atomic scale due to the factor  $u_v^* u_c$ , which is periodic with the crystal lattice.

In conclusion, we have demonstrated the complete failure of the atomic picture for interband dipole moments and charge oscillation in real quantum-well systems. It is essential that terms from at least two band edges are used in an envelope-function approximation when performing such calculations.

R.A.C. would like to thank EPSRC and BT for financial support.

- <sup>1</sup>M. G. Burt, J. Phys.: Condens. Matter **5**, 4091 (1993).
- <sup>2</sup>M. G. Burt, Superlattices Microstruct. **17**, 335 (1995).
- <sup>3</sup>M. G. Burt, Semicond. Sci. Technol. **10**, 412 (1995).
- <sup>4</sup>M. L. Cohen and T. K. Bergstresser, Phys. Rev. **141**, 789 (1966).
- <sup>5</sup>M. L. Cohen and J. R. Chelikowsky, *Electronic Structure and Optical Properties of Semiconductors* (Springer-Verlag, Berlin, 1988).
- <sup>6</sup>Y.-C. Chang and J. N. Schulman, Phys. Rev. B **25**, 3975 (1982).
- <sup>7</sup>S. Brand and D. T. Hughes, Semicond. Sci. Technol. **2**, 607 (1987).
- <sup>8</sup>M. G. Burt, J. Phys.: Condens. Matter **4**, 6651 (1992).
- <sup>9</sup>S. Adachi, *Physical Properties of III-V Semiconductor Compounds* (Wiley, New York, 1992).
- <sup>10</sup>A. C. G. Wood, Ph.D. thesis, University of Durham, 1990 (unpublished).
- <sup>11</sup>D. L. Smith and C. Mailhot, Rev. Mod. Phys. **62**, 173 (1990).
- <sup>12</sup>Y.-C. Chang and J. N. Schulman, Phys. Rev. B **31**, 2069 (1985).
- <sup>13</sup>L. C. West and S. J. Eglash, Appl. Phys. Lett. **46**, 1156 (1985).
- <sup>14</sup>K. J. Mackey *et al.*, Appl. Phys. Lett. **49**, 354 (1986).
- <sup>15</sup>A. Qteish and R. J. Needs, Phys. Rev. B **47**, 3714 (1993).